THE JOURNAL OF PHYSICAL CHEMISTRY B

ARTICLE

pubs.acs.org/JPCB

Interactions of Phosphororganic Agents with Water and Components of Polyelectrolyte Membranes

Ming-Tsung Lee, Aleksey Vishnyakov, Gennady Yu. Gor, and Alexander V. Neimark*

Department of Chemical and Biochemical Engineering, Rutgers, The State University of New Jersey, 98 Brett Road, Piscataway, New Jersey 08854, United States

Supporting Information

ABSTRACT: Interactions of nerve G-agents (sarin and soman) and their simulants DMMP (dimethyl methylphosphonate) and DIFP (diisopropyl fluorophosphate) with water and components of polyelectrolyte membranes are studied using ab initio calculations in conjunction with thermodynamic modeling using the conductor-like screening model for real solvents (COSMO-RS). To test reliability of COSMO-RS calculations, we measured the vapor−liquid equilibrium in DMMP−water mixtures and found quantitative agreement between computed and experimental results. Using COSMO-RS, we studied the interactions of phosphororganic agents with the characteristic fragments of perfluorinated and sulfonated polystyrene (sPS) polyelectrolytes, which are explored for protective clothing membranes. We found that both simulants, DIFP and DMMP, mimic the thermodynamic properties of G-agents reasonably well; however, there are certain specific differences that are discussed. We also suggested that sPS-based polyelectrolytes have less affinity for phosphorganic agents compared to prefluorinated polyelectrolytes similar to Nafion.

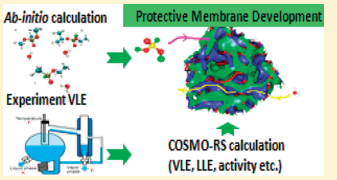

I. INTRODUCTION

The interest in a better understanding of the specific interactions of phosphororganic compounds and water with sulfonated polystyrene (sPS) and sulfonated fluoropolymers is motivated by their potential use as protective barriers against chemical warfare agents (CWAs). Because of their extreme toxicity, CWAs are often mimicked in experiments by simulants, that is, similar compounds of low toxicity whose chemistry and transport properties are close to those of CWAs. G-agents soman and sarin are routinely simulated by dimethyl methylphosphonate (DMMP) and diisopropyl fluorophosphate (DIFP)[1−3] shown in Figure 1. Being structurally similar to G-agents, they do not include the "core" methylflourophosphonate group, which is substituted by methylphosphonate and fluorophosphate groups in DMMP and DIFP, respectively. As such, either fluorine or the methyl group at the phosporus atom of a G-agent is replaced by an alkoxy group in the simulants. It is worth noting that DMMP is a low-toxicity compound with a wide range of industrial applications, while DIFP is by itself a potent neurotoxin, although much weaker than G-agents.

Unlike phosphates, which are found in biological macromolecules, aqueous solutions of alkylphosphonates and fluorophosphates received relatively little attention from both experimentalists and theoreticians. First published studies of thermodynamic and dielectric properties of lower alkylphosphonates including DMMP date back to 1950s.[4−7] The dielectric constants obtained allowed to speculate on preferential conformations of lower alkylphosphonates: in particular, "extended" and "folded" geometries were considered.[4,6] Dipole moments of lower alkylphosphonates were estimated from the dielectric constants using the Onsager model; in particular, the dipole moment of 3.62D was reported for DMMP.[6]

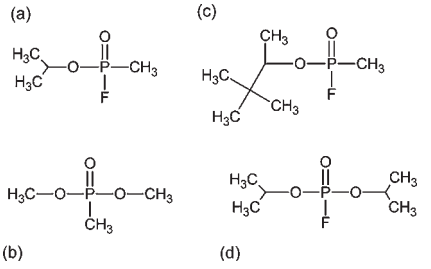

Figure 1. Chemical structures of phosphororganic chemicals considered in this paper: (a) sarin (GB, *O*-isopropyl methylphosphonofluoridate, an organophosphorous CWA), (b) dimethyl methylphosphonate (DMMP, simulant for G-agents), (c) soman (GD, *O*-pinacolyl methylphosphonofluoridate, an organophosphorous CWA), (d) diisopropylfluorophosphate (DIFP, a simulant for G-agents).

Vapor−liquid equilibria (VLE) for individual phosphorogranic agents were studied in refs 8 and 9. Butrow et al.[10] measured the vapor pressure, volatility, and heat of evaporation of four lower alkyl phosphonate compounds including DMMP. Theoretical studies of G-agents and their simulants were mostly conducted at the ab initio level. In particular, Suenram et al. thoroughly studied the conformations of DMMP, sarin and soman molecules in vacuum using restricted Hartree−Fock (RHF) and Møller−Plesset (MP2) perturbation theory[11] calculations in conjunction with Fourier transform microwave spectroscopy.[12−14] Kaczmarek et al.[15] determined the most stable conformers of sarin and soman in high-level-correlated calculations

Received: August 4, 2011
Revised: October 5, 2011
Published: October 12, 2011

with extended Gaussian basis sets. Cuisset et al.[16] performed the MP2[17] and the B3LYP[18−21] (Becke, 3-parameter, Lee−Yang−Parr) version of the density functional theory (DFT) ab initio calculations on the two lowest energy conformers of DMMP, comparing to the experimental values measured by gas phase vibrational spectroscopy. Mamaev et al.[22] studied dynamic structure of four fluorophosphonates, including sarin and soman. Their quantum chemical calculations were made by semiempirical SCF (self-consistent field) AM1 (Austin model) method and RHF method with 3-21 G* basis set, comparing the literature results of MP2, DFT and experimental gas-phase electron diffraction data. Majumdar et al.[23] carried out conformational analysis of sarin and soman at the DFT-B3LYP/6-31++G(d,p) level, comparing to MP2 with 6-31++G** results and experimental values. Stukov et al.[24] used AM1 method in studying O-alkyl methylfluorophosphonates. Bermudez provided a series of ab initio calculations to describe DMMP adsorption on various surfaces.[25−30] On the basis of these ab initio and experimental studies, atomistic force fields for classical simulations were developed for DMMP and G-agents,[31,32] and a good agreement with pure component saturation pressures was achieved.[31]

Published results on multicomponent systems that include the compounds of interest are limited. Compilation of most of the experimental data was given by Bizzigotti et al.[33,34] and by Bartelt-Hunt et al.[35] who reviewed the densities, vapor pressures, and solubilities of selected phosphororganic chemicals. These authors discussed the appropriate choice of nerve agent simulants and the influence of these physicochemical properties on the fate, transport, and environmental impact of chemical agents in marine environments. Tevault et al.[36] measured the dew points of bicomponent vapors composed of DMMP and water. There are also a few theoretical studies of DMMP−water mixtures. Ault et al.[37] considered DMMP interactions with water using infrared spectra obtained experimentally and in ab initio calculations. Vishnyakov et al. employed molecular dynamics simulations to explore thermodynamics and structure of aqueous solutions of DMMP, DIFP, sarin, and soman as well as polyelectrolyte solvation on DMMP−water mixtures.[32,38]

The work presented here is motivated by the practical need of a better understanding of interactions of toxic agents with polyelectrolyte membranes (PEMs) explored for the design of novel protective clothing materials. We suggest to employ the conductor-like screening model for thermodynamic calculations (COSMO-RS),[39] combined with ab initio optimization for comparative analyses of interactions of selected chemical warfare agents and their simulants with typical components of hydrated polyelectrolyte membranes. We pursue three purposes: (1) explore the interactions of alkylphosphonate CWAs and their simulants with water, (2) test the ability of COSMO-RS to reproduce the experimental data for the systems of interest, and (3) understand how well the simulants (DMMP and DIFP) mimic the actual G-agents in different aspects that may be relevant to their capture by PEMs. In order to validate the proposed approach, we compared the results of calculations with the experimental data and available literature data on previous computational studies on interactions of agents with water. Due to the lack of experimental data, we have measured the experimental VLE phase diagrams of aqueous solution of DMMP. This piece of experimental work has its own value and was included as a special section. Good agreement of calculated and experimental data served as a proof that COSMO-RS is a promising tool for studies of agent/simulant aqueous systems of our interest. After such validation, COSMO-RS was then used to study the systems for which experimental data are not available and to analyze with computations to what extent the simulants may mimic agent interactions with typical ionic components of polyeletrolyte membranes. This new physical insight is instrumental for intelligent design of novel protective materials from polyelecrolyte membranes.

The paper is organized as follows. The results of ab initio optimization of agents and simulants and the study of hydrogen bond formation with water molecules are presented in section II. This information provides an insight onto the structural similarity of simulants and agents and their interactions with water, and is employed to produce the input data of COSMO-RS calculations. The experimental study of VLE in aqueous solutions of DMMP is described in section III. The results of COSMO-RS calculations of agent-water and simulant-water VLE and their comparison with the experimental data from section III and the literature are given in section IV. Section V presents the analysis of the interactions of agents and simulants with typical ionic components of polyelectrolyte membranes, which dominate membrane sorption properties. A summary of the obtained results is given in section VI. The Supporting Information includes (I) experimental procedure to measure the DMMP−water VLE, (II) attempt to model the VLE using Peng−Robinson cubic equation of state, (III) examination of vapor phase nonideality by correcting the VLE diagrams obtained by COSMO-RS using the Peng−Robinson equation, and (IV) σ profiles of G-agents and the stimulants used in COSMO-RS calculations.

II. VACUUM OPTIMIZATION OF G-AGENTS AND SIMULANTS AND HYDROGEN BONDING TO WATER MOLECULE

Before studying interactions between chemical and water we minimized the four molecules under consideration (soman, sarin, DMMP, and DIFP) in vacuum using the density functional theory (DFT) with B3LYP exchange-correlation functional in the standard split-valence 6-311++G(2d,2p) basis set. The choice of the B3LYP functional is justified by its previous successful use for calculations of DMMP-water hydrogen bond formation and IR spectra by Ault et al.,[37] which will be discussed later in this section. First, we searched the conformational space of each molecule in order to identify all potentially stable conformers with Accelrys Materials Studio[40] using classical Universal forcefield,[41] and then the identified conformers were subjected to further ab initio optimization, which was performed with PQS ab initio software package.[42,43] We obtained all stable conformations of sarin, DMMP, and DIFP and probable minimum-energy conformations of soman. From the population analysis, we estimated the dipole moments and partial charges using the CHELPG algorithm. Our conformations are in good agreement with those reported in the literature,[13,15] as well as the dipole moment of lowest energy conformers. In particular, for sarin we obtained four conformers with the dipole moments of the lowest three equal to 3.44, 3.43, and 3.31 D. The lowest three conformers reported by Kaczmarek et al.[15] are almost identical to ours and the dipole moments are slightly lower. In similar MP2/6-311G** calculations of Walker et al.,[14] the dipoles were closer to our calculations (3.29 and 3.27 D for the two lowest conformers), while their experimental estimate showed a weaker overall dipole of 1.73 D. Our dipole moments of 3.11 and 3.09 D for the SS and SR diastereomers of soman are comparable with

Table 1. Molecular Characteristics of Sarin, Soman, and Two Simulants DMMP and DIFP[a]

compound	p, D	$\langle p \rangle$, D	ΔE, kcal/mol	l_H, Å	O···H−O angle, deg	q_O, e	q_F, e	$\Delta\nu_{O-H}$
DMMP	2.21	2.17	−7.06 (7.52)	1.861	167.6	−0.65		−202
sarin	3.44	3.44	−6.41 (6.90)	1.882	165.1	−0.62	−0.23	−171
DIFP	1.56	2.29	−6.25 (6.83)	1.897	164.1	−0.53	−0.14	−166
soman	3.09	3.10	−6.22 (6.72)	1.935	159.8	−0.57	−0.25	−157

[a] Columns as follows: p, dipole moment in minimum-energy conformation; $\langle p \rangle$, Boltzmann-weighted average for all stable conformers at 298 K; ΔE, energies of complexation of each phosphororganic chemical with a single water molecule (the values in brackets are uncorrected values with BSSE included); l_H, length of hydrogen bond donated by water to the double-bonded O(=P) oxygen, in Å, O···H−O angle in degrees; q_O, charges of the O(=P) oxygen obtained with CHELPG method; q_F, fluorine partial charge; $\Delta\nu_{O-H}$, shifts of characteristic IR frequency (symmetrical stretching of O−H bond in water) compared to that in a single water molecule in vacuum. According to Ault et al.[37] ΔE = −7.7 kcal/mol (MP2 calculations) and $\Delta\nu_{O-H}$ = −203 cm^{-1}. For details, see section II.

the results obtained by RHF (3.00 and 2.98 D) and MP2 modeling (3.10 and 3.07 D) in ref 15. However, Suenram et al.[12] reported considerably stronger dipoles of 3.60 and 3.61 D. Same trend was observed for DMMP: our conformers were similar to those obtained by Suenram et al.[13] with MP2 with slightly weaker dipoles. It is worth noting that DMMP dipole moments obtained from the dielectric properties using the Onsager model were also quite high (3.62 D),[6] although these values cannot be expected to coincide with the single molecule dipole moments in vacuum.

In all these molecules, the positive charge is concentrated on the central phosphorus atom and on the carbon(s) attached to the "ether" oxygen in P−O−C fragments. This charge is effectively compensated by the negative charge on the O(=P) oxygen that forms a double bond with the phosphorus, and the fluorine, where available. Therefore, the dipole moment that largely determines the dielectric properties and significantly influences diffusion in polyelectrolytes, strongly depends on the conformation. Taking in account most stable conformations, we can determine the "Boltzmann weighted average" for the dipoles of the G-agents and simulants and the intervals, within which their dipoles vary. Among the four compounds considered, sarin has the highest dipole moment; however, it is DMMP that shows the most negative charge on the O(=P) oxygen. The partial negative charge of the fluorine atom in sarin and DIFP is significantly smaller than the charge of O(=P) oxygen in both cases (see Table 1).

To characterize the interactions of G-agents and simulants with water, we evaluated the energy of formation of complexes with single water molecule (Figure 2). The latter was placed in the vicinity of O(=P) oxygen so that it could donate a hydrogen bond to the agent molecule. Then the energy of this complex formation was calculated taking in account the basis set superposition error (BSSE) via the standard counterpoise procedure.[44] We verified that the results did not depend on the initial position of the water molecule.

The energies of complex formation are given in Table 1. Energy values are given after BSSE correction. The uncorrected values, which include the artificial BSSE term, are given in brackets. The corrected complexation energies are close to the typical energies of O−H···O hydrogen bonds (e.g., the value reported for liquid water in ref 45 was −5.58 kcal/mol), and we may expect that in aqueous solution, the O(=P) oxygen, is about as attractive as a hydrogen bond acceptor as the water oxygen. DMMP forms the strongest hydrogen bond with water, stronger than the G-agents, and DIFP forms a weaker bond; the respective values follow the same trend as the partial charge on the O(=P) atom calculated using CHELPG[46] orbital population analysis.

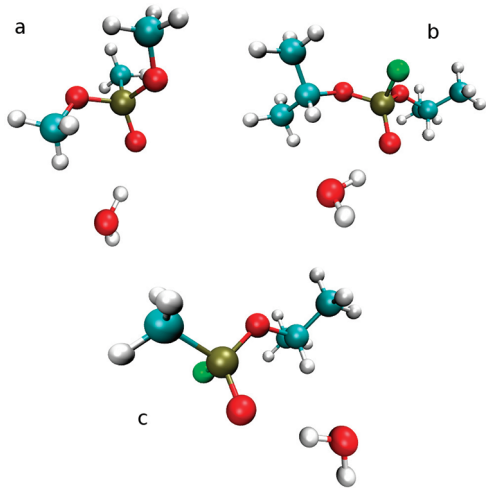

Figure 2. Conformations with lowest energy of DMMP (a), DIFP (b), and sarin (c) complexes with water minimized using DFT in B3LYP exchange correlation functional and 6-311++G(2d,2p) basis set. References for color of atom: Hydrogen in white, oxygen in red, fluorine in green, carbon in blue, and phosphorus in brown.

Because the complexation energies do not necessarily represent those of hydrogen bonds, we also calculated the infrared (IR) spectra of isolated molecules and complexes. We obtained the values for the red shift of O−H symmetric stretching mode for the water molecule hydrogen. From Table 1, one can see that the larger is the negative atomic charge of double-bonded oxygen, the stronger is the hydrogen bond, the shorter is the length of hydrogen bond, and the higher is the corresponding shift of O−H stretching frequency.

For DMMP·H_2O complex formation, the ab initio studies were performed before using various levels of theory, along with matrix-isolation experiments.[37] Although different methods in quantum chemical calculation may bring a sufficient differences in H-bonding energy,[47] our purpose is browsing the similarity between simulant and G-agent and their interaction with water using the same method. We use standard split-valence basis set, and our values for both ΔE and $\Delta\nu_{O-H}$ for DMMP are close to the experimental values reported in ref 37. For binding energy of DMMP and water, Ault et al. reported it as −7.7 kcal/mol at the MP2/6-31+G** level including the counterpoise correction. We have −7.52 kcal/mol with B3LYP 6-311++G(2d, 2p) basis set, and −7.06 kcal/mol accounting the basis set superposition error. Experimental observation of O−H stretching in the work by

Ault et al.[37] has the shift of −203 cm^{-1} upon the formation of hydrogen bond. Our calculations have the value at −202 cm^{-1} correspondingly. Our choice of using DFT/B3LYP was then justified by the quantitatively reproducing MP2 results and experimental values in this previously successful study for DMMP and water interaction. Nevertheless, it should be also aware that one should consider the cooperativity effect of water clustering in studying systems with hydrogen bonding as in ref 48. This is a substantial work, which is beyond the scope of this paper. In addition, the validation of our calculations was built comparing to the work by Ault et al.,[37] where their study was restricted to one DMMP and one water molecule.

III. EXPERIMENTAL MEASUREMENTS OF VAPOR−LIQUID EQUILIBRIUM DIAGRAMS FOR DMMP−WATER BINARY SYSTEM

Because of a relative scarcity and uncertainties of published experimental data, we measured vapor−liquid phase diagrams for DMMP−water system using an Othmer Still distillation column. The experimental details are given in the Supporting Information, section 1. Measurements were done at the pressures of p = 0.226 and 0.331 atm. At atmospheric pressure, we approximately measured the boiling temperatures only. The pressure substantially below 1 atm was necessary to bring the boiling temperature down thus avoiding DMMP hydrolysis, which is non-negligible at the atmospheric pressure as determined by NMR analysis (see the Supporting Information, Figure S3)

A sample of ca. 250 mL of a binary solution was placed into a flask. The solution was heated to bring it to boiling. Vapor evaporating from the flask condensed in a cooler and was collected in a collector. As soon as the vapor temperature measured using an RTD thermometer stabilized and remained constant (that means that the equilibrium between vapor and liquid phases had established), the portion of the distillate from the collector was discarded, and boiling proceeded until we collected a portion of ca. 3 mL. After that, the samples of both phases (liquid from the flask and vapor from the collector) were placed in vials and left overnight to cool to the lab temperature. Then the densities and refractive indexes of the samples collected were measured and interpolated onto the density-composition and refractive-indexes-composition reference curves (given in the Supporting Information Figure S1).

IV. PREDICTIONS OF VLE AND LLE FOR THE MIXTURES OF PHOSPHORORGANIC AGENTS WITH WATER WITH COSMO-RS

Although knowledge of the interactions between individual molecules in vacuum is useful, it is not sufficient to understand the behavior of complex systems such as hydrated PEMs. We attempted to characterize the interactions between G-agents and simulants with the ionic components of selected PEMs using COSMO-RS thermodynamic model. Conductor-like screening model (COSMO)[49] is designed to obtain the total energy of the solute in a virtual conductor as well as the screening charge density on the molecular surface using DFT. Then the interactions in the target fluid are described as local contact interactions of the charged segments of the molecular surfaces. Thus, the ensemble of interacting molecules is approximated by an ensemble of independently interacting surface segments. Dispersion interactions

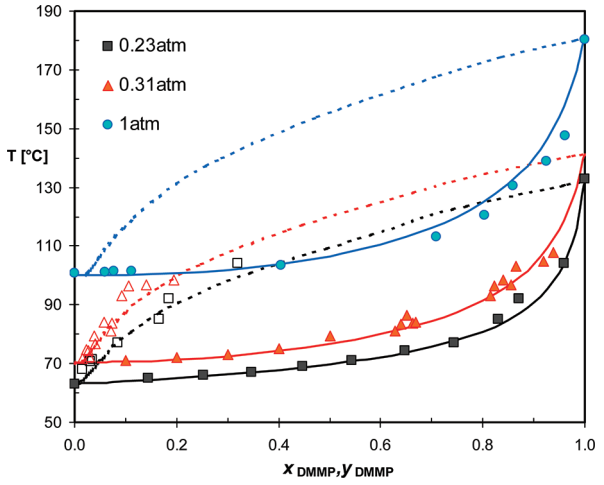

Figure 3. Constant pressure *Txy* vapor−liquid phase diagrams for DMMP−water system at pressure equals to 0.226 (black), 0.311 (red), and 1 atm (blue). Symbols represent our experimental measurements, with filled symbols for liquid phase and open symbols for vapor phase. Lines represent COSMO-RS modeling, with solid lines for liquid phase and dashed lines for vapor phase. The lack of vapor phase experimental data at 1 atm, and for y_{DMMP} larger than 0.3 at 0.226 and 0.31 atm was due to technical difficulties (see Supporting Information).

are modeled in a more approximate fashion. COSMO-RS,[39] based on the perfect screening of solute molecule and the calculations for the deviation between the ideality and real solvent, is used in variety of studies of solvation phenomena. The statistico-thermodynamic formalism of COSMO-RS approach allows for calculation of the effective chemical potentials of the molecule segments, out of which the free energy of liquid, and therefore, the chemical potential of the components may be derived. COSMO-RS generally demonstrates a good agreement with thermodynamic properties of polar compounds and appears to suit our systems well. We tested COSMO-RS against our experimental results and selected results from the literature.

In our calculations of the VLE diagrams for DMMP-water system, we supposed that DMMP in aqueous solutions assumes two main conformations described by Suenram et al.[13] and checked that these two conformers are the optimal ones under COSMO as well. The charge screening profiles (see the Supporting Information, Figure S7) obtained with PQS ab initio software were used in COSMO-RS calculations of component activity coefficients using COSMO*therm*,[50] assuming Boltzmann-weighted distribution between different conformers. Phase equilibrium calculations by COSMO-RS rely on the statistical consideration of the charge density profile of molecules. For vapor liquid equilibrium calculations in COSMO*therm*, vapor phase behavior was assumed ideal. We have also modeled the water-DMMP VLE using the Peng−Robinson cubic EOS at one atmosphere (which is the highest pressure in our VLE study) and came to a conclusion that vapor nonideality has a miniscule influence on the phase diagram (see Figure S6 in the Supporting Information) . The ideal gas assumption in vapor phase of COSMO*therm* is valid at one atmosphere pressure and below.

Figure 3 depicts the experimental and theoretical VLE diagrams of DMMP-water binary system at constant pressures (p) of 0.226, 0.311, and 1 atm. The abscissa shows the mole fractions of DMMP x_{DMMP} in the equilibrium liquid and vapor and

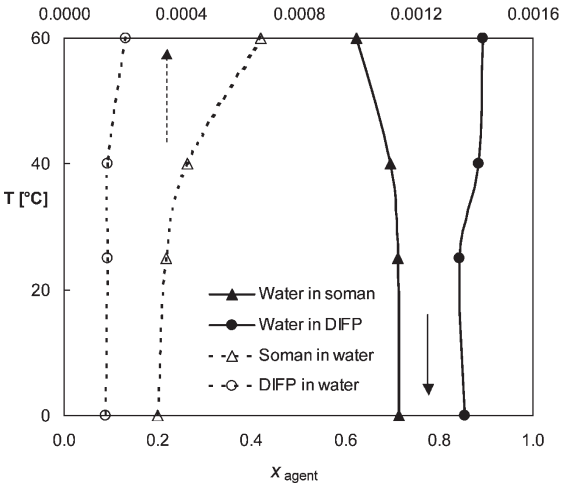

Figure 4. COSMO-RS liquid−liquid equilibrium calculations for mutual solubilities of soman (lines with triangles) and DIFP (lines with circles) with water at 0, 25, 40, and 60 °C. Solid lines with filled symbols are water solubilities in soman/DIFP-rich phase, referring to the bottom primary abscissa (0−1). Dashed lines with open symbols are soman/DIFP solubilities in water-rich phase (0−0.0016), referring to the upper secondary abscissa. Literature experimental data were collected in the section IV for comparison.

the ordinate shows the equilibrium boiling temperature for each composition. So, if one draws a horizontal line crossing the ordinate at temperature T, the intersections of this line with the liquid and vapor branches give us DMMP mole fractions in the equilibrium liquid and vapor $x_{DMMP}(T)$ and $y_{DMMP}(T)$ The experimental VLE diagrams have a standard shape showing no visible azeotrope or liquid-phase separation (Figure 3). Overall, COSMO−RS predictions agree quantitatively with our experiments. In the liquid phase, components are fully miscible, in accord with the experiments. COSMO-RS predicts barely visible minimum-temperature azeotropes at all pressures. At p = 1 atm, the azeotropic point corresponds to x_{DMMP} = 0.01 and lies 0.03 K below the pure water boiling temperature. At p = 0.226 atm, the azeotrope is predicted at T = 336.15 K and x_{DMMP} = 0.00001. The precision of our experiments is insufficient to judge whether the azeotropisc points do exist in water-DMMP mixture, because the azeotrope is practically undetectable at p = 0.226 and 0.311 atm, and we could not obtain the vapor curve at p = 1 atm because of DMMP hydrolysis.

Another test for COSMO-RS is the prediction of LLE for phosphororganic compounds, using the literature data for soman and DIFP.[35] Figure 4 presents mutual solubilities of soman and DIFP with water at 0, 25, 40, and 60 °C calculated using COSMO-RS. We performed the activity coefficient calculations for soman/DIFP and water binary mixtures, and sought the compositions for soman/DIFP and water where the chemical potential in agent-rich phase and in water-rich phase are equal. Both soman and DIFP have limited solubility in water (dashed lines refer to upper abscissa in Figure 4), although water solubility in both agents is substantial (solid lines refer to lower abscissa in Figure 4). COSMO-RS does correctly reproduce this nontrivial behavior, predicting 4.1% and 1.3% water mass fraction of water in soman-rich and DIFP-rich liquid phases, correspondingly. Interestingly, the solubility of water in soman changes very little as the temperature increases, and COSMO-RS also reproduces this effect well. However, the solubilities of soman in water are significantly underestimated by the COSMO-RS model that predicts 4.3 and 1.5 g of water per 1 L of soman and DIFP, correspondingly, vs 21 and 15 g/L obtained in published experiments.[35]

V. INTERACTION OF G-AGENTS AND SIMULANTS WITH THE IONIC COMPONENTS OF SELECT POLYELECTROLYTE MEMBRANES

Having obtained reasonable agreement between COSMO-RS and experiments for selected binary systems of water and phosphororganic agents, we attempted to describe the interactions of those agents with the components of PEMs using activity coefficients in model macroscopic solutions. The polyelectrolytes of interest consist of hydrophobic and hydrophilic fragments. In Nafion, a perfluoroether chain terminated by a sulfonate group is attached to fluorocarbon skeleton. In partially sulfonated polysterene, the hydrophilic fragment is the sulfonated benzene ring, while the hydrophobic fragments include the alkane backbone and unsulfonated phenyls. At high level of hydration, the hydrophilic terminal chains are surrounded by water clusters. That is why we expect that activity coefficients of G-agents and simulants in aqueous solutions containing the ionic groups of the polyelectrolytes provide useful information on the interactions between these chemicals and the same groups in the hydrophilic subphases of segregated PEMs.

We modeled the ammonium triflate (trifluoromethanesulfonate) $CF_3SO_3^-NH_4^+$ and ammonium benzenesulfonate $C_6H_5SO_3^-NH_4^+$. Ammonium counterion was selected because of its convenience in COSMO calculations. The procedure was as follows: we created virtual mixtures of water and one of the phosphororganic compounds. Then, keeping the molar ratio of water to organic component constant, we increased the molality of electrolyte from zero to 1 m. A shift in the activity coefficient of an agent characterizes its interaction with the anion. Deviations of electrolyte molality dependences between the agent and its simulant demonstrate the difference in their interactions with the polyelectrolyte side chains

Figure 5 shows the activity coefficients γ of G-agents and simulants in the solutions containing $CF_3SO_3^-$ and $PhSO_3^-$ anions at different water-to-chemical ratios. Interestingly, the concentration of the triflate anion does not have much influence on the activity coefficient of sarin for all three water-to-sarin ratios considered. At 1:10 and 1:5 sarin:water ratios, the activity coefficient of sarin increases slowly and monotonically with the $NH_4CF_3SO_3$ concentration. In dilute (1:100) sarin solutions, however, $\gamma(m)$ for sarin passes through a peculiar maximum at about 0.5. But overall, sarin vapor pressure for sarin−water−$NH_4CF_3SO_3$ solutions would be close to those for sarin-water solutions at the same sarin-to-water ratio.

Activity coefficients of DMMP are generally lower than those of sarin at the same concentrations, which is consistent with DMMP being more hydrophilic. Interestingly, $\gamma(m)$ passes a maximum for DMMP as well, but overall, the activity coefficients steeply decrease when ammonium triflate is added, which signifies that interactions between DMMP and the triflate anion are very favorable and facilitate DMMP sorption in hydrated perfluorinated polymers of Nafion type. The qualitative deviation from sarin behavior also leads to a conclusion that sorption results for DMMP should not be automatically projected onto sarin behavior, but at the same time DMMP would probably be

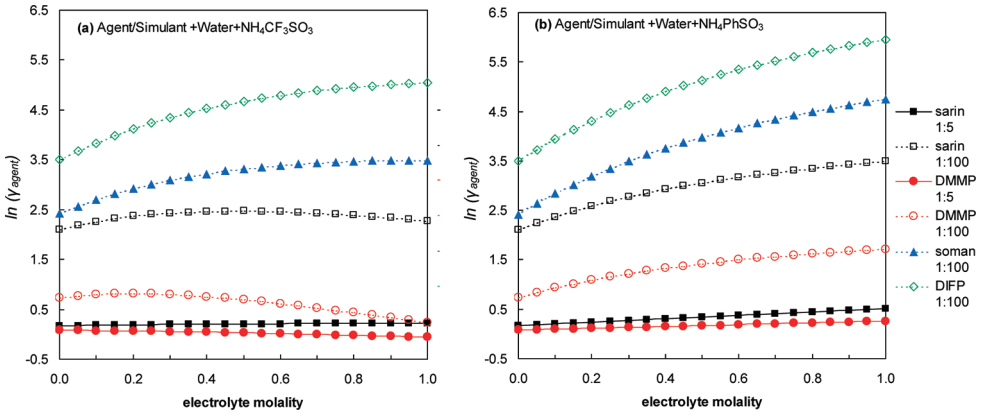

Figure 5. Logarithm of activity coefficients of G-agents and simulants in the solutions containing (a) $NH_4CF_3SO_3$ and (b) NH_4PhSO_3 versus electrolyte molality at different water-to-chemical ratios, showing the favorable tendencies of agents/simulants with different membranes and in different hydration levels. Solid lines are for 1:5, long dashed lines are for 1:10, and short dashed lines are for 1:100 chemical-to-water ratio. Different colors represent the chemical: sarin (black), DMMP (red), soman (blue), and DIFP (green).

absorbed better and diffuse faster (exactly due to a better sorption) compared to sarin. In contrast, DIFP activity coefficients in water are higher than those of sarin and increase monotonically with the electrolyte concentration.

When ammonium triflate is replaced by benzenesulfonate, the behavior of DMMP changes. Like all other chemicals considered, DMMP shows a monotonic increase of the activity coefficient with the molality of the electrolyte. Furthermore, the increase of activity coefficient with the electrolyte molality is much steeper in ammonium benzenesulfonate solutions compared to the ammonium triflate solutions, indicating that the interactions and triflate anion with the organophosphorous chemicals considered here are much less favorable.

VI. CONCLUSION

The COSMO-RS method is shown to be a suitable tool for prediction of the properties of phosphororganic agents in aqueous environments. It provides reasonable agreement with experimental data on VLE and LLE of aqueous solutions of alkylphosphonates and fluorophsphoates. The experimental data of VLE of DMMP-water solutions were collected specifically to test the computation results.

Quantum chemical calculations by DFT/B3LYP with 6-311+G-(2d,2p) were employed to study the chemical structural similarity between simulants and agents, and their interactions with water. The binding energy and shifts of characteristic IR frequency of DMMP and water are in agreement with MP2/6-31 +G** calculations and experimental values by Ault et al.[37] that validates the reliability of our ab initio calculations, including the generation of molecular charge surfaces used as input in COSMO-RS calculations.

To get a better understanding of simulants in mimicking agents with the hydrated membranes, we studied the interactions between simulants and agents with characteristic membrane components that determine the membrane sorption properties. The results of modeling of the interactions of G-agents with the ionic components of PEMs, represented by triflate and benzenesulfonate anions, showed substantial differences, which may have significant implications in terms of the prospective use of polyelectrolytes as protective barrier materials. Benzenesulfonate ion appears to interact unfavorably (compared to the triflate) with G-agents and simulants alike, especially at low concentration of the phosphororganic component. For triflate ion, there is no obvious influence of the electrolyte molality on the agent−ion interactions, whereas DMMP interacts favorably with the triflate. As such, sPS based PEMs may have a better potential for applications in protective materials compared to perfluorinated PEMs.

In general, it appears that alkylphosphonates and fluorophosphates mimic the interactions of G-agents with water reasonably well, which is indicated by the characteristics of hydrogen bonding between water and those phosphororganic chemicals, such as complexation energy and vibrational frequencies. Alkylphosphonates displayed stronger hydrophilicity compared to G-agents, contrary to fluorophosphates, which are more hydrophobic. Comparison of the activity coefficient of G-agents and their simulants in the model solutions suggests that fluorophosphates mimic the behavior of G-agents better than the alkylphosphonates of similar size. On the other hand, alkylphosphonates are preferred to fluorophosphates because of a substantial toxicity of the latter.

■ ASSOCIATED CONTENT

Supporting Information. Description of experimental procedure for obtaining VLE for DMMP-water mixture, calibration curves for DMMP-water density-composition and refractive index-composition dependences. This material is available free of charge via the Internet at http://pubs.acs.org.

■ AUTHOR INFORMATION

Corresponding Author
*E-mail: aneimark@rci.rutgers.edu.

■ ACKNOWLEDGMENT

We thank John Landers for helpful advice regarding experimental part of the paper and Michael Drahl for conducting NMR analysis. This work was supported by in parts by DTRA Grant HDTRA1-08-1-0042 and ARO Grant W911NF-09-1-0242.

REFERENCES

(1) Frishman, G.; Amirav, A. *Field Anal. Chem. Technol.* **2000**, *4*, 170–194.
(2) Suzin, Y.; Nir, I.; Kaplan, D. *Carbon* **2000**, *38*, 1129–1133.
(3) Vo-Dinh, T.; Stokes, D. L. *Field Anal. Chem. Technol.* **1999**, *3*, 346–356.
(4) Arbuzov, B. A.; Shavsha, T. G. *Izv. Akad. Nauk Arm. SSR, Ser. Khim.* **1952**, 875–881.
(5) Arbuzov, B. A.; Vinogradova, V. S. *Izv. Akad. Nauk Arm. SSR, Ser. Khim.* **1952**, 865–874.
(6) Kosolapoff, G. M. *J. Chem. Soc.* **1954**, 3222–3225.
(7) Kosolapoff, G. M. *J. Am. Chem. Soc.* **1954**, *76*, 615–617.
(8) Buchanan, J. H.; Sumpter, K. B.; Abercrombie, P. L.; Tevault, D. E. "Vapor Pressure of GB," U. S. Army Edgewood Biological Center: Aberdeen Proving Ground, MD, 2009.
(9) Balboa, A.; Buchanan, J. H.; Buettner, L. C.; Sewell, S.; Tevault, D. E. "Vapor Pressure of GD," U. S. Army Edgewood Biological Center: Aberdeen Proving Ground, MD, 2007.
(10) Butrow, A. B.; Buchanan, J. H.; Tevault, D. E. *J. Chem. Eng. Data* **2009**, *54*, 1876–1883.
(11) Moller, C.; Plesset, M. S. *Phys. Rev.* **1934**, *46*, 0618–0622.
(12) Suenram, R. D.; DaBell, R. S.; Walker, A. R. H.; Lavrich, R. J.; Plusquellic, D. F.; Ellzy, M. W.; Lochner, J. M.; Cash, L.; Jensen, J. O.; Samuels, A. C. *J. Mol. Spectrosc.* **2004**, *224*, 176–184.
(13) Suenram, R. D.; Lovas, F. J.; Plusquellic, D. F.; Lesarri, A.; Kawashima, Y.; Jensen, J. O.; Samuels, A. C. *J. Mol. Spectrosc.* **2002**, *211*, 110–118.
(14) Walker, A. R. H.; Suenram, R. D.; Samuels, A.; Jensen, J.; Ellzy, M. W.; Lochner, J. M.; Zeroka, D. *J. Mol. Spectrosc.* **2001**, *207*, 77–82.
(15) Kaczmarek, A.; Gorb, L.; Sadlej, A. J.; Leszczynski, J. *Struct. Chem.* **2004**, *15*, 517–525.
(16) Cuisset, A.; Mouret, G.; Pirali, O.; Roy, P.; Cazier, F.; Nouali, H.; Demaison, J. *J. Phys. Chem. B* **2008**, *112*, 12516–12525.
(17) Headgordon, M.; Pople, J. A.; Frisch, M. J. *Chem. Phys. Lett.* **1988**, *153*, 503–506.
(18) Becke, A. D. *J. Chem. Phys.* **1993**, *98*, 5648–5652.
(19) Lee, C. T.; Yang, W. T.; Parr, R. G. *Phys. Rev. B* **1988**, *37*, 785–789.
(20) Stephens, P. J.; Devlin, F. J.; Chabalowski, C. F.; Frisch, M. J. *J. Phys. Chem.* **1994**, *98*, 11623–11627.
(21) Vosko, S. H.; Wilk, L.; Nusair, M. *Can. J. Phys.* **1980**, *58*, 1200–1211.
(22) Mamaev, V. M.; Zernova, E. V.; Prisyazhnyuk, A. V.; Myshakin, E. M.; Berdyshev, D. V. *Dokl. Akad. Nauk* **1996**, *349*, 64–66.
(23) Majumdar, D.; Roszakz, S.; Leszczynski, J. *Mol. Phys.* **2007**, *105*, 2551–2564.
(24) Strukov, O. G.; Utkina, S. V.; Petrunin, V. A.; Vlasova, Z. V.; Zavalishina, I. V.; Fadeev, V. N.; Kuntsevich, A. D.; Drozd, G. I. *Doklady Phys. Chem.* **2001**, *380*, 247–253.
(25) Bermudez, V. M. *J. Phys. Chem. C* **2007**, *111*, 3719–3728.
(26) Bermudez, V. M. *J. Phys. Chem. C* **2007**, *111*, 9314–9323.
(27) Bermudez, V. M. *J. Phys. Chem. C* **2009**, *113*, 1917–1930.
(28) Bermudez, V. M. *J. Phys. Chem. C* **2010**, *114*, 3063–3074.
(29) Bermudez, V. M. *Langmuir* **2010**, *26*, 18144–18154.
(30) Bermudez, V. M. *Surf. Sci.* **2010**, *604*, 706–712.
(31) Sokkalingam, N.; Kamath, G.; Coscione, M.; Potoff, J. J. *J. Phys. Chem. B* **2009**, *113*, 10292–10297.
(32) Vishnyakov, A.; Gor, G. Y.; Lee, M.-T.; Neimark, A. V. *J. Phys. Chem. A* **2011**, *115*, 5201–5209.
(33) Bizzigotti, G.; Castelly, H.; Hafez, A.; Smith, W.; Whitmire, M. *Chem. Rev.* **2010**, *110*, 3850–3850.
(34) Bizzigotti, G. O.; Castelly, H.; Hafez, A. M.; Smith, W. H. B.; Whitmire, M. T. *Chem. Rev.* **2009**, *109*, 236–256.
(35) Bartelt-Hunt, S. L.; Knappe, D. R. U.; Barlaz, M. A. *Crit. Rev. Environ. Sci. Technol.* **2008**, *38*, 112–136.
(36) Tevault, D. E.; Buchanan, J. H.; Buettner, L. C. *Int. J. Thermophys.* **2006**, *27*, 486–493.
(37) Ault, B. S.; Balboa, A.; Tevault, D.; Hurley, M. *J. Phys. Chem. A* **2004**, *108*, 10094–10098.
(38) Vishnyakov, A.; Neimark, A. V. *J. Phys. Chem. A* **2004**, *108*, 1435–1439.
(39) Klamt, A. *J. Phys. Chem.* **1995**, *99*, 2224–2235.
(40) Materials Studio; version 4.2.; Accelrys: San Diego, 2007.
(41) Rappe, A. K.; Casewit, C. J.; Colwell, K. S.; Goddard, W. A.; Skiff, W. M. *J. Am. Chem. Soc.* **1992**, *114*, 10024–10035.
(42) Pulay, P.; Baker, J.; Wolinski, K. PQS ab initio; 3.3 ed.; Parallel Quantum Solutions: Fayetteville, AR, 2003.
(43) Baker, J.; Wolinski, K.; Malagoli, M.; Kinghorn, D.; Wolinski, P.; Magyarfalvi, G.; Saebo, S.; Janowski, T.; Pulay, P. *J. Comput. Chem.* **2009**, *30*, 317–335.
(44) Boys, S. F.; Bernardi, F. The calculation of small molecular interactions by the differences of separate total energies. Some procedures with reduced errors; Taylor & Francis: London, 1970; Vol. 19; pp 553−566.
(45) Suresh, S. J.; Naik, V. M. *J. Chem. Phys.* **2000**, *113*, 9727–9732.
(46) Breneman, C. M.; Wiberg, K. B. *J. Comput. Chem.* **1990**, *11*, 361–373.
(47) Thanthiriwatte, K. S.; Hohenstein, E. G.; Burns, L. A.; Sherrill, C. D. *J. Chem. Theory Comput.* **2011**, *7*, 88–96.
(48) Pavlov, M.; Siegbahn, P. E. M.; Sandstrom, M. *J. Phys. Chem. A* **1998**, *102*, 219–228.
(49) Klamt, A.; Schuurmann, G. *J. Chem. Soc.-Perkin Trans. 2* **1993**, 799–805.
(50) COSMO*therm*, version. C2.1; COSMOlogic GmbH: Leverkusen, 2003.